Substrate specificity, plasma membrane localization, and lipid modification of the aldehyde dehydrogenase ALDH3B1

Takuya Kitamura, Tatsuro Naganuma, Kensuke Abe, Kanae Nakahara, Yusuke Ohno, Akio Kihara*

Laboratory of Biochemistry, Faculty of Pharmaceutical Sciences, Hokkaido University, Sapporo, Japan

*Corresponding author

Address correspondence to:

Akio Kihara

Laboratory of Biochemistry

Faculty of Pharmaceutical Sciences, Hokkaido University

Kita 12-jo, Nishi 6-chome, Kita-ku, Sapporo 060-0812, Japan

Telephone: +81-11-706-3754

Fax: +81-11-706-4900

E-mail: kihara@pharm.hokudai.ac.jp

Abstract

The accumulation of reactive aldehydes is implicated in the development of several disorders. Aldehyde dehydrogenases (ALDHs) detoxify aldehydes by oxidizing them to the corresponding carboxylic acids. Among the 19 human ALDHs, ALDH3A2 is the only known ALDH that catalyzes the oxidation of long-chain fatty aldehydes including C16 aldehydes (hexadecanal and *trans*-2-hexadecenal) generated through sphingolipid metabolism. In the present study, we have identified that ALDH3B1 is also active *in vitro* toward C16 aldehydes and demonstrated that overexpression of ALDH3B1 restores the sphingolipid metabolism in the *ALDH3A2*-deficient cells. In addition, we have determined that ALDH3B1 is localized in the plasma membrane through its C-terminal dual lipidation (palmitoylation and prenylation) and shown that the prenylation is required particularly for the activity toward hexadecanal. Since knockdown of *ALDH3B1* does not cause further impairment of the sphingolipid metabolism in the *ALDH3A2*-deficient cells, the likely physiological function of ALDH3B1 is to oxidize lipid-derived aldehydes generated in the plasma membrane and not to be involved in the sphingolipid metabolism in the endoplasmic reticulum.

Keywords: aldehyde/ aldehyde dehydrogenase/ sphingolipid/ plasma membrane/ prenylation/ palmitoylation

Abbreviations: ABE, acyl-biotinyl exchange; ALDH, aldehyde dehydrogenase; Cer, ceramide; DHS, dihydrosphingosine; ER, endoplasmic reticulum; GlcCer, glucosylceramide; IPC, inositol phosphorylceramide; LCB, long-chain base; MIPC,

mannosylinositol phosphorylceramide; $M(IP)_2C$, mannosyldiinositol phosphorylceramide; PC, phosphatidylcholine; PE, phosphatidylethanolamine; PI, phosphatidylinositol; PlsC, plasmanylcholine; PlsE, plasmenylethanolamine; PS, phosphatidylserine; S1P, sphingosine 1-phoshosphate; SM, sphingomyelin.

1. Introduction

A wide variety of aldehydes are generated in the organism from endogenous and exogenous substrates such as lipids, amino acids, and neurotransmitters, as well as foods, drugs, and pollutants [1]. Being highly reactive molecules, the accumulation of aldehydes often has toxic effects on cells. Aldehyde dehydrogenases (ALDHs) are a group of enzymes that catalyze the oxidation of aldehydes to less reactive carboxylic acids, thus alleviating the aldehyde-induced cytotoxicity. There are 19 ALDHs known in humans with different substrate specificity, tissue distribution, and intracellular localization [1]. Mutations in these *ALDH* genes and consequent aldehyde accumulation have been implicated in the pathogenesis of several inherited diseases, including Sjögren-Larsson syndrome (*ALDH3A2*) [2], type II hyperprolinemia (*ALDH4A1*) [3], pyridoxine-dependent seizures (*ALDH7A1*) [4], and γ-hydroxybutyric aciduria (*ALDH5A1*) [5].

The mammalian ALDH3 subfamily is comprised of ALDH3A1, ALDH3A2, ALDH3B1, and ALDH3B2, which share sequence similarity. ALDH3A1 is a highly expressed corneal soluble protein and protects the cornea and underlying lens against UV-induced oxidative stress (as lipid peroxidation) by eliminating the toxic aldehydes including 4-hydroxy-2-nonenal [6]. ALDH3A2 is expressed ubiquitously and exhibits activity toward aliphatic aldehydes of C6 to C24 [7], such as those derived from dietary phytol [8], leukotriene B_4 [9], and sphingosine 1-phoshosphate (S1P) [10]. Two splicing isoforms of ALDH3A2 are known: a major isoform localized in the endoplasmic reticulum (ER) and a minor isoform in the peroxisomes [11]. ALDH3B1 is expressed in the kidney, liver, and brain and has been shown active *in vitro* toward C6 to C9 aldehydes [12]; however, its activity toward ≥C10 aldehydes is currently unknown. In addition, although

ALDH3B1 is suggested to be localized in the plasma membrane and cytosol [13, 14], the precise intracellular localization still remains to be elucidated. Unlike other ALDH3 family members, ALDH3B2 has so far not been well characterized.

We recently reported the involvement of ALDH3A2 in the metabolism of sphingolipid-derived C16 aldehydes to glycerophospholipids [10]. Sphingolipids and glycerophospholipids are major lipid components of the eukaryotic plasma membrane. The hydrophobic backbone of sphingolipids is a ceramide (Cer) composed of a long-chain base (LCB) and an amide-linked fatty acid [15]. In mammals, the major LCB is sphingosine with a *trans* double bond between the 4th and 5th carbons, accompanied by the saturated analogue dihydrosphingosine (DHS). These LCBs are phosphorylated by sphingosine kinases to the LCB 1-phosphates (S1P and DHS 1-phosphate) and further degrade by S1P lyase to phosphoethanolamine and the corresponding C16 aldehydes (*trans*-2-hexadecenal and hexadecanal, respectively) [15]. The generated C16 aldehydes are subsequently oxidized by ALDH3A2 and are eventually metabolized to glycerophospholipids [10]. Interestingly, during our investigation, we noticed that the *ALDH3A2*-mutant CHO-K1 cells (FAA-K1A) were still able to metabolize LCBs to glycerophospholipids, albeit to a lesser extent compared to the wild-type CHO-K1 cells. We therefore suspected that another ALDH might be responsible for the residual activity [10].

So far, ALDH3A2 is the only known ALDH that exhibits activity toward C16 aldehydes. In the present study, we have identified ALDH3B1 as another ALDH3 family member capable of oxidizing C16 aldehydes and biochemically characterized its substrate specificity, intracellular localization, and lipid modification.

2. Material and methods

2.1. Cell culture and transfection

HEK 293T and HeLa cells were grown in Dulbecco's modified Eagle's medium (Sigma, St. Louis, MO) and CHO-K1 cells in Ham's F-12 medium (Sigma), with each medium supplemented with 10% fetal bovine serum, 100 units/ml penicillin, and 100 μg/ml streptomycin. HEK 293T cells were grown in dishes coated with 0.3% collagen. The *ALDH3A2*-null FAA-K1A cells were described previously [10, 16]. Transfections were performed using Lipofectamine Plus^{TM} Reagent (Invitrogen, Carlsbad, CA) according to the manufacturer's instructions.

2.2. Yeast strains and media

The yeast *Saccharomyces cerevisiae* strain BY4741 (*MAT**a** his3Δ1 leu2Δ0 met15Δ0 ura3Δ0*) [17] and its Δ*hfd1::KanMX4* derivative (strain 6550) [18] were obtained from Open Biosystems (Huntsville, AL). Cells were grown in either YPD medium (1% yeast extract, 2% bactopeptone, and 2% D-glucose) or synthetic complete medium lacking uracil (0.67% yeast nitrogen base, 2% D-glucose, 0.5 % casamino acids, 20 mg/l adenine, and 20 mg/l tryptophan).

2.3. Plasmids

The pCE-puro 3xFLAG-1 [19], pCE-puro His_6-Myc-1 [19], and pEGFP-C1 (Clontech, TAKARA Bio, Palo Alto, CA) plasmids are mammalian expression vectors designed to produce proteins tagged with an N-terminal 3xFLAG, an N-terminal tandemly oriented His_6 and Myc epitope (His_6-Myc), and an N-terminal enhanced GFP protein, respectively. The

pAKNF316 (*URA3* marker) plasmid is a yeast expression vector designed to produce an N-terminal 3xFLAG-tagged protein [10]. The plasmids encoding *3xFLAG*-tagged human *ALDH3A2* cDNA (pCE-puro 3xFLAG-ALDH3A2 for expression in mammalian cells and pNK5 for expression in yeast) were described previously [10].

The human *ALDH3A1*, *ALDH3B1*, and *ALDH3B2* cDNAs were amplified by PCR using appropriate templates (for *ALDH3A1*, human EST clone ID 3610317 (Thermo Fisher Scientific, Waltham, MA); for *ALDH3B1*, human lung cDNA (Clontech, TAKARA Bio); and for *ALDH3B2*, human placenta cDNA (Clontech, TAKARA Bio)) and primers (for *ALDH3A1*, 5'-TCTAGAATGAGCAAGATCAGCGAGGCCGTGA-3' (*Xba*I site underlined) and 5'-TCAGTGCTGGGTCATCTTGGCCGGG-3'; for *ALDH3B1*, 5'-GGATCCATGGACCCCCTTGGGGACACGCTG-3' (*Bam*HI site underlined) and 5'-TCAGAGCAGTGTGCAGCTGCAGCC-3'; and for *ALDH3B2*, 5'-GGATCCATGAAGGATGAACCACGGTCCACG-3' (*Bam*HI site underlined) and 5'-GGATCCTCACAGGAGGGTGCAGCTCTGGGAG-3' (*Bam*HI site underlined)). The amplified fragments were first cloned into the pGEM-T Easy vector (Promega, Madison, WI). The cDNA fragment was then prepared from each resulting plasmid by digesting with appropriate restriction enzymes and cloned into the pAKNF316, pCE-puro 3xFLAG-1, or pCE-puro His_6-Myc-1 vector. The pNK10 (*3xFLAG-ALDH3A1*), pNK12 (*3xFLAG-ALDH3B1*), and pNK14 (*3xFLAG-ALDH3B2*) plasmids were derived from the pAKNF316 plasmid. The pCE-puro 3xFLAG-ALDH3A1, pCE-puro 3xFLAG-ALDH3B1, pCE-puro His_6-Myc-ALDH3B1, and pCE-puro 3xFLAG-ALDH3B2 plasmids were constructed using either pCE-puro 3xFLAG-1 or pCE-puro His_6-Myc-1 vector.

The plasmids encoding *ALDH3B1* mutants (*C463S*, *C465S*, and *C463/465S*) were

constructed using QuikChange site-directed mutagenesis kit (Stratagene, Agilent Technologies, La Jolla, CA) with primers (for *C463S*, 5'-CCATGGAGGCCCAAGGCTCCAGCTGCACACTGCTC-3' and 5'-GAGCAGTGTGCAGCTGGAGCCTTGGGCCTCCATGG-3'; for *C465S*, 5'-GGAGGCCCAAGGCTGCAGCTCCACACTGCTCTG-3' and 5'-CAGAGCAGTGTGGAGCTGCAGCCTTGGGCCTCC-3'; and for *C463/465S*, 5'-GGAGGCCCAAGGCTCCAGCTCCACACTGCTCTG-3' and 5'-CAGAGCAGTGTGGAGCTGGAGCCTTGGGCCTCC-3'). The wild-type and *ALDH3B1* mutant cDNAs were cloned into the following vectors: the pCE-puro 3xFLAG-1 vector to produce the pCE-puro 3xFLAG-ALDH3B1-C463S, pCE-puro 3xFLAG-ALDH3B1-C465S, and pCE-puro 3xFLAG-ALDH3B1-C463/465S plasmids; the pEGFP-C1 vector to generate the pEGFP-ALDH3B1, pEGFP-ALDH3B1-C463S, pEGFP-ALDH3B1-C465S, and pEGFP-ALDH3B1-C463/465S plasmids; and the pAKNF316 vector to create the pTK71 (*3xFLAG-ALDH3B1-C463/465S*) plasmid.

2.4. [^{3}H]DHS labeling assay

The assay was performed using [4,5-^{3}H]DHS (50 Ci/mmol; American Radiolabeled Chemicals, St Louis, MO) as described previously [10].

2.5. Production of stable transformants of FAA-K1A cells

To obtain FAA-K1A derivatives stably expressing the human ALDH3B1 protein, the pCE-puro His_6-Myc-ALDH3B1 plasmid was transfected into FAA-K1A cells. The transfected cells were subjected to selection in 10 μg/ml puromycin for 10 days. The

FAA-ALDH3B1-A and FAA-ALDH3B1-B cells expressing the highest level of His_6-Myc-ALDH3B1 were used for further analyses.

2.6. Immunoblotting

Immunoblotting was performed as described previously [20] using anti-FLAG (M2; 1 μg/ml; Stratagene), anti-Myc (9E10; 1 μg/ml; Enzo Life Sciences, Farmingdale, NY), anti-calnexin (H-10; 0.2 μg/ml; Santa Cruz Biotechnology, Santa Cruz, CA), anti-GAPDH (1 μg/ml; Ambion, Austin, TX), and anti-Pgk1 (0.25 μg/ml; Molecular Probes, Invitrogen, Eugene, OR) as the primary antibodies and HRP-conjugated anti-rabbit and anti-mouse IgG $F(ab')_2$ fragment (each 1:7500 dilution; GE Healthcare Life Sciences, Buckinghamshire, UK) as the secondary antibodies. Labeling was detected using Pierce Western Blotting Substrate (Thermo Fisher Scientific).

2.7. Cell fractionation

Cells treated with or without the geranylgeranyltransferase I inhibitor GGTI-2133 (Sigma) were suspended in buffer A (50 mM HEPES-NaOH (pH 7.4), 150 mM NaCl, 10% glycerol, 1 mM dithiothreitol, 1 mM phenylmethylsulfonyl fluoride, and 1X Complete™ protease inhibitor mixture (EDTA-free; Roche Diagnostics, Indianapolis, IN)) and lysed by sonication. Unlysed cells and aggregated proteins were removed by centrifugation at 20,400 x g for 5 min. The supernatant (total lysate) was centrifuged at 100,000 x g for 30 min at 4 ˚C, and the resulting pellet (membrane fraction) and supernatant (soluble fraction) were subjected to immunoblotting.

2.8. In vitro ALDH assay

3xFLAG-ALDH3A1, 3xFLAG-ALDH3A2, 3xFLAG-ALDH3B1, 3xFLAG-ALDH3B2, and 3xFLAG-ALDH3B1 lipidation mutants (C463S, C465S, and C463/465S) were expressed in HEK 293T cells and affinity-purified using anti-FLAG M2 affinity agarose gel as described previously [10].

The assay was performed using hexadecanal [21], *trans*-2-hexadecenal (Avanti Polar Lipid, Alabaster, AL), and octanal (Wako Pure Chemical Industries, Osaka, Japan) as substrates. The affinity-purified protein (10-20 ng) was incubated with 500 μM NAD^+ and 100 μM aldehyde in 50 μl buffer B (50 mM Tris-HCl (pH 8.5), 150 mM NaCl, 10% glycerol, and 0.1% Triton X-100) at 37 ˚C. The reaction was monitored by measuring the fluorescence of the NADH product (excitation at 356 nm and emission at 460 nm) using monochromator Infinite M200 (Tecan, Männedorf, Switzerland). A linear standard curve was obtained from 0, 5, 10, and 25 μM of NADH and used to quantify the NADH produced in the assay.

2.9. Acyl-biotinyl exchange (ABE) assay

The assay was performed as described previously [22].

3. Results

3.1. ALDH3B1 exhibits activity toward hexadecanal

We first used yeast Δ*hfd1* cells to identify an additional ALDH3 family member with ALDH3A2-like activity toward C16 aldehydes (Fig. 1). Hfd1 is the yeast ALDH responsible for the oxidation of LCB-derived hexadecanal and *trans*-2-hexadecenal and, therefore, the yeast Δ*hfd1* cells are incapable of metabolizing LCBs to glycerophospholipids [10]. The human *ALDH3* genes (*ALDH3A1*, *ALDH3A2*, *ALDH3B1*, and *ALDH3B2*) were cloned and introduced separately into the Δ*hfd1* cells. We then investigated the recovery of LCB-to-glycerophospholipid metabolism by monitoring the fate of exogenously added [^{3}H]DHS in each cell. In Δ*hfd1* cells bearing the vector control, [^{3}H]DHS was converted to sphingolipids (inositol phosphorylceramide (IPC), mannosylinositol phosphorylceramide (MIPC), and mannosyldiinositol phosphorylceramide ($M(IP)_2C$)) but not to glycerophospholipids (phosphatidylethanolamine (PE), phosphatidylcholine (PC), phosphatidylserine (PS), and phosphatidylinositol (PI)) (Fig. 1A). In contrast, cells harboring the plasmid encoding either *ALDH3A2* or *ALDH3B1* metabolized [^{3}H]DHS to both sphingolipids and glycerophospholipids. Neither *ALDH3A1* nor *ALDH3B2* could restore the DHS-to-glycerophospholipid metabolism, although their protein levels were comparable to both ALDH3A2 and ALDH3B1 levels (Fig. 1B). These findings suggest that, like ALDH3A2, ALDH3B1 functions as ALDH in the Δ*hfd1* cells oxidizing hexadecanal derived from DHS.

We next employed mammalian CHO-K1 cells deficient in ALDH3A2 (FAA-K1A cells) to examine if ALDH3B1 compensates the function of the missing ALDH3A2 (Fig. 2). In CHO-K1 cells, [^{3}H]DHS is metabolized to both sphingolipids (Cer, sphingomyelin (SM),

and glucosylceramide (GlcCer)) and glycerophospholipids (PE, PC, PS, and PI). However, FAA-K1A cells reduce the DHS-to-glycerophospholipid conversion and, instead, produce ether-linked glycerophospholipids (plasmenylethanolamine (PlsE) and plasmanylcholine (PlsC)) [10] (Fig. 2A). We generated two independent FAA-K1A cell lines stably expressing His_6-Myc-tagged ALDH3B1 at a similar level (FAA-ALDH3B1-A and FAA-ALDH3B1-B cells) (Fig. 2B). In both stable cell lines, the glycerophospholipid level was restored to the level found in the CHO-K1 cells without the formation of the ether-linked glycerophospholipids (Fig. 2A). Thus, overexpressed ALDH3B1 is able to substitute for ALDH3A2 in the oxidation of hexadecanal derived from DHS.

3.2. ALDH3B1 exhibits activity toward C16 aldehydes

We further assessed the *in vitro* activity of ALDH3B1 using 3xFLAG-tagged ALDH3 proteins, expressed in HEK 293T cells and affinity purified with anti-FLAG antibody-conjugated agarose beads. Both ALDH3B1 and ALDH3A2 exhibited high activity toward hexadecanal; however, the activity of ALDH3A1 and ALDH3B2 was low (Fig. 3A). The findings are consistent with the yeast cell results (Fig. 1A).

Using 3xFLAG-ALDH3B1, we determined kinetic parameters for ALDH3B1-catalyzed oxidation of hexadecanal (Fig. 3B), *trans*-2-hexadecenal (Fig. 3C), and octanal (Fig. 3D). The V_{max} (pmol/min/ng protein) and K_m (μM) values were found to be 9.7 and 45.6 (hexadecanal), 4.8 and 4.9 (hexadecenal), and 5.0 and 25.0 (octanal), respectively. Thus, ALDH3B1 has a similar V_{max} for these aldehyde substrates; however, the lowest K_m for hexadecenal indicates its highest affinity toward hexadecenal.

3.3. ALDH3B1 is dually lipidated

To determine the precise intracellular localization of ALDH3B1, we fractionated the total cell lysate prepared from HeLa cells expressing 3xFLAG-ALDH3B1 into soluble and membrane fractions and found most of ALDH3B1 in the membrane fraction (Fig. 4A). Since ALDH3B1 has no apparent transmembrane domain, lipid modification was thought to facilitate membrane association. Prenylation involves the addition of either a C15 farnesyl or a C20 geranylgeranyl isoprenoid moiety to the Cys residue in the C-terminal CaaX prenylation motif (where "C" is prenylated Cys and "a" is an aliphatic amino acid). The X residue determines the type of prenylation: farnesylation (X = Ser, Met, Gln, or Cys) or geranylgeranylation (X = Leu or Ile) [23]. The Cys residues near the prenylated Cys residue are also often palmitoylated [23]. ALDH3B1 contains the C-terminal CSCTLL sequence where Cys463 and Cys465 are potential palmitoylation and prenylation sites, respectively (Fig. 4B). We therefore evaluated the effect of the geranylgeranyltransferase I inhibitor GGTI-2133 on the membrane localization of ALDH3B1. Upon treatment with GGTI-2133, ALDH3B1 showed a dose-dependent shift from the membrane fraction to the soluble fraction (Fig. 4A). These findings suggest that ALDH3B1 is localized to the membranes via geranylgeranylation.

Next, we examined the possibility of palmitoylation by performing an acyl-biotinyl exchange (ABE) assay, which substitutes biotin for the palmitate moiety [24]. Successful introduction of the biotin label indicated that ALDH3B1 is indeed palmitoylated (Fig. 4C). To confirm the involvement of the predicted palmitoylation site Cys463, we created the Ser-substituted mutant (C463S). We also produced a mutant of the prenylated Cys residue (C465S) and the double-lipidation mutant (C463/465S). Palmitoylation of ALDH3B1 was

abolished in both C463S and C463/465S mutants (Fig. 4C), indicative of Cys463 residue being the palmitoylation site. Moreover, significantly reduced palmitoylation of the C465S mutant suggested that prenylation is required for subsequent palmitoylation.

3.4. Lipid modification of ALDH3B1 is important for its plasma membrane localization and activity toward hexadecanal

We further investigated the role of this lipidation in the intracellular localization and function of ALDH3B1. To monitor the localization, the N-terminally EGFP-tagged wild-type and mutant ALDH3B1 proteins were expressed in HeLa cells (Fig. 5A). Although EGFP alone was localized in the cytosol and nucleus, the wild-type EGFP-ALDH3B1 was found primarily in the plasma membrane as well as in some punctate structures in the cytoplasm. A similar localization pattern was observed for the palmitoylation mutant (C463S). In contrast, the prenylation mutant (C465S) and the double-lipidation mutant (C463/465S) were found to be localized in the cytosol. These results substantiate that prenylation is essential for the plasma membrane localization of ALDH3B1.

We also examined the membrane localization of the lipidation mutants by cell fractionation (Fig. 5B). Only 62% of the palmitoylation mutant (C463S) was found in the membrane fraction, which was interesting since the intracellular localization of this mutant was not detected by fluorescence microscopy (Fig. 5A). The prenylation mutant (C465S) was mainly recovered in the soluble fraction (65%), and the level of localization in the soluble fraction was further increased to 82% by the additional palmitoylation mutation (C463/465S). Considering ~90% of the wild-type ALDH3B1 found in the membrane fraction, palmitoylation is certainly an additional requirement for the membrane localization

of ALDH3B1.

Given the plasma membrane localization of ALDH3B1, although overexpression of ALDH3B1 restored the deficient LCB metabolism in FAA-K1A cells (Fig. 2A), it is not likely that the normally-expressed ALDH3B1 is responsible for the residual LCB metabolism in FAA-K1A cells since LCB metabolism occurs in the ER. To confirm this notion, we performed knockdown analysis of *ALDH3B1* in FAA-K1A cells. While the level of *ALDH3B1* mRNA was efficiently reduced (Fig. S1A), the conversion of [^{3}H]DHS to glycerophospholipids was not further decreased; rather, the PE/PlsE level was slightly increased compared to the control knockdown cells (Fig. S1B). Thus, ALDH3B1 appears not to be involved in the LCB metabolism in FAA-K1A cells under the normal condition.

Finally, we evaluated the ALDH activity of each lipidation mutant (Fig. 6A). The wild type and the mutants showed a similar activity toward octanal. The activity toward hexadecanal was comparable between the wild-type ALDH3B1 and the C463S mutant; however, both C465S and C463/465S mutants showed a significantly lower activity. When the C463/465S mutant was expressed in the Δ*hfd1* cells, the DHS-to-glycerophospholipid conversion was only partially recovered (Fig. 6B). The expression of the mutant protein was found similar to the wild type (Fig. 6C). Thus, prenylation of ALDH3B1 is important for the oxidation of hexadecanal both *in vitro* and at the cellular level.

4. Discussion

The human genome contains 19 *ALDH* genes [1]. This high multiplicity may be needed to detoxify reactive aldehydes generated in tissues and intracellular organelles from various endogenous and exogenous sources. To understand the overall mechanism of aldehyde detoxification in the organism, each ALDH needs to be fully characterized in terms of its substrate specificity, tissue distribution, and intracellular localization. ALDH3B1 is one of the ALDHs whose full characterization has not yet been completed. In the present study, we have revealed that ALDH3B1 is active toward C16 aldehydes both *in vitro* and in cells (yeast and mammalian cells) (Figs. 1, 2, and 3). Since the activity toward C6 to C9 aldehydes is reported [12], ALDH3B1 is considered to be capable of oxidizing a broad range of medium- to long-chain aliphatic aldehydes.

In this respect, the substrate specificity of ALDH3B1 resembles that of ALDH3A2 [7] . We have found that ALDH3B1 is localized in the plasma membrane (Fig. 5A), while ALDH3A2 is present mainly in the ER [11]. Therefore, these two ALDH3 family members are responsible for the oxidation of lipid-derived aldehydes in distinct organelles. For example, the LCB-derived C16 aldehydes are generated in the ER [25] and thereby detoxified primarily by ALDH3A2 and not by ALDH3B1. Indeed, the *ALDH3B1* knockdown has no effect on the residual metabolism of DHS to glycerophospholipids in FAA-K1A cells (Fig. S1). However, overexpression of ALDH3B1 in both yeast Δ*hfd1* and mammalian FAA-K1A cells resulted in the recovery of the deficient DHS-to-glycerophospholipid metabolism (Figs. 1A and 2A). To account for this finding, we speculate that overexpression of ALDH3B1 might increase the level of newly synthesized ER-resident ALDH3B1 enough to oxidize the LCB-derived C16 aldehydes in the ER. In the

plasma membrane, the unsaturated fatty acids in glycerophospholipids as well as the vinyl ether linkage in plasmalogens are susceptible to oxidative stress-induced lipid peroxidation generating aldehydes [26, 27]. Therefore, it is highly likely that ALDH3B1 plays a major role in the detoxification of these aldehydes. Indeed, the protective function of ALDH3B1 against oxidative stress has been reported [14].

As other many prenylated proteins such as Ras and Rho GTPases [28], ALDH3B1 was found to be dually lipidated (palmitoylation and prenylation). It is reported that, whereas prenylation only promotes a transient membrane interaction, the additional palmitoylation promotes the stable association [29, 30]. The majority of the wild-type ALDH3B1 (dually lipidated) was recovered in the membrane fraction, yet a significant amount of the singly lipidated palmitoylation and prenylatioin mutants (C463S and C465S) were found in the soluble fraction (Fig. 5B). Thus, the dual lipidation appears to allow ALDH3B1 to stably associate with the plasma membrane. Such lipid modification has never been reported for ALDHs.

Post-translational modification of Ras GTPase proceeds via prenylation followed by palmitoylation [31, 32]. The decreased level of palmitoylation is reported for the prenylation mutant of Rac1 and yeast Ras [31, 32]. Likewise, palmitoylation of the prenylation mutant C465S was greatly decreased (Fig. 4C). It is possible that prenylation of ALDH3B1 induces its membrane association and/or conformational changes required for the palmitoyltransferase recognition.

The prenylation site mutation was also found to affect the activity of ALDH3B1 toward hexadecanal but not octanal (Fig. 6A). Hexadecanal is much more hydrophobic than octanal and is likely to associate with the membrane or the micelle of the non-ionic

detergent used in our *in vitro* assay. Therefore, the membrane or micelle association of ALDH3B1 through prenylation may be required for the efficient recognition of hexadecanal.

Recently, a single nucleotide polymorphism in the *ALDH3B1* gene has been identified to be responsible for the pathogenesis of paranoid schizophrenia [33, 34]. Aldehydes and their associated toxicity are implicated in various disorders, including cataract, cutaneous disorder, cancer, neuronal diseases, alcoholic liver disease, and male infertility [1-4, 35-38]. To understand the molecular and cellular mechanisms underlying the pathology of these disorders, the identification of disease-causative aldehydes and the characterization of yet uncharacterized ALDHs will be required in future studies.

Acknowledgements: This work was supported by Grants-in-Aid for Scientific Research on Innovative Areas (23116701 and 25117701) from the Ministry of Education, Culture, Sports, Sciences and Technology of Japan. We are grateful to Professor R. A. Zoeller (Boston University School of Medicine) providing the for FAA-K1A cells. We also thank Dr. T. Toyokuni for scientific editing of the manuscript.

References

[1] S.A. Marchitti, C. Brocker, D. Stagos, V. Vasiliou, Non-P450 aldehyde oxidizing enzymes: the aldehyde dehydrogenase superfamily, Expert Opin. Drug. Metab. Toxicol. 4 (2008) 697-720.

[2] W.B. Rizzo, Sjögren-Larsson syndrome: molecular genetics and biochemical pathogenesis of fatty aldehyde dehydrogenase deficiency, Mol. Genet. Metab. 90 (2007) 1-9.

[3] M.T. Geraghty, D. Vaughn, A.J. Nicholson, W.W. Lin, G. Jimenez-Sanchez, C. Obie, M.P. Flynn, D. Valle, C.A. Hu, Mutations in the Δ^1-pyrroline 5-carboxylate dehydrogenase gene cause type II hyperprolinemia, Hum. Mol. Genet. 7 (1998) 1411-1415.

[4] P.B. Mills, E. Struys, C. Jakobs, B. Plecko, P. Baxter, M. Baumgartner, M.A. Willemsen, H. Omran, U. Tacke, B. Uhlenberg, B. Weschke, P.T. Clayton, Mutations in antiquitin in individuals with pyridoxine-dependent seizures, Nat. Med. 12 (2006) 307-309.

[5] S. Akaboshi, B.M. Hogema, A. Novelletto, P. Malaspina, G.S. Salomons, G.D. Maropoulos, C. Jakobs, M. Grompe, K.M. Gibson, Mutational spectrum of the succinate semialdehyde dehydrogenase (*ALDH5A1*) gene and functional analysis of 27 novel disease-causing mutations in patients with SSADH deficiency, Hum. Mutat. 22 (2003) 442-450.

[6] T. Estey, J. Piatigorsky, N. Lassen, V. Vasiliou, ALDH3A1: a corneal crystallin with diverse functions, Exp. Eye Res. 84 (2007) 3-12.

[7] T.L. Kelson, J.R. Secor McVoy, W.B. Rizzo, Human liver fatty aldehyde

dehydrogenase: microsomal localization, purification, and biochemical characterization, Biochim. Biophys. Acta 1335 (1997) 99-110.

[8] N.M. Verhoeven, C. Jakobs, G. Carney, M.P. Somers, R.J. Wanders, W.B. Rizzo, Involvement of microsomal fatty aldehyde dehydrogenase in the α-oxidation of phytanic acid, FEBS Lett. 429 (1998) 225-228.

[9] M.A. Willemsen, J.J. Rotteveel, J.G. de Jong, R.J. Wanders, I.J. L, G.F. Hoffmann, E. Mayatepek, Defective metabolism of leukotriene B_4 in the Sjögren-Larsson syndrome, J. Neurol. Sci. 183 (2001) 61-67.

[10] K. Nakahara, A. Ohkuni, T. Kitamura, K. Abe, T. Naganuma, Y. Ohno, R.A. Zoeller, A. Kihara, The Sjögren-Larsson syndrome gene encodes a hexadecenal dehydrogenase of the sphingosine 1-phosphate degradation pathway, Mol. Cell 46 (2012) 461-471.

[11] B. Ashibe, T. Hirai, K. Higashi, K. Sekimizu, K. Motojima, Dual subcellular localization in the endoplasmic reticulum and peroxisomes and a vital role in protecting against oxidative stress of fatty aldehyde dehydrogenase are achieved by alternative splicing, J. Biol. Chem. 282 (2007) 20763-20773.

[12] S.A. Marchitti, D.J. Orlicky, V. Vasiliou, Expression and initial characterization of human ALDH3B1, Biochem. Biophys. Res. Commun. 356 (2007) 792-798.

[13] S.A. Marchitti, D.J. Orlicky, C. Brocker, V. Vasiliou, Aldehyde dehydrogenase 3B1 (ALDH3B1): immunohistochemical tissue distribution and cellular-specific localization in normal and cancerous human tissues, J. Histochem. Cytochem. 58 (2010) 765-783.

[14] S.A. Marchitti, C. Brocker, D.J. Orlicky, V. Vasiliou, Molecular characterization,

expression analysis, and role of ALDH3B1 in the cellular protection against oxidative stress, Free Radic. Biol. Med. 49 (2010) 1432-1443.

[15] A. Kihara, S. Mitsutake, Y. Mizutani, Y. Igarashi, Metabolism and biological functions of two phosphorylated sphingolipids, sphingosine 1-phosphate and ceramide 1-phosphate, Prog. Lipid Res. 46 (2007) 126-144.

[16] P.F. James, R.A. Zoeller, Isolation of animal cell mutants defective in long-chain fatty aldehyde dehydrogenase. Sensitivity to fatty aldehydes and Schiff's base modification of phospholipids: implications for Sjögren-Larsson syndrome, J. Biol. Chem. 272 (1997) 23532-23539.

[17] C.B. Brachmann, A. Davies, G.J. Cost, E. Caputo, J. Li, P. Hieter, J.D. Boeke, Designer deletion strains derived from *Saccharomyces cerevisiae* S288C: a useful set of strains and plasmids for PCR-mediated gene disruption and other applications, Yeast 14 (1998) 115-132.

[18] E.A. Winzeler, D.D. Shoemaker, A. Astromoff, H. Liang, K. Anderson, B. Andre, R. Bangham, R. Benito, J.D. Boeke, H. Bussey, A.M. Chu, C. Connelly, K. Davis, F. Dietrich, S.W. Dow, M. El Bakkoury, F. Foury, S.H. Friend, E. Gentalen, G. Giaever, J.H. Hegemann, T. Jones, M. Laub, H. Liao, N. Liebundguth, D.J. Lockhart, A. Lucau-Danila, M. Lussier, N. M'Rabet, P. Menard, M. Mittmann, C. Pai, C. Rebischung, J.L. Revuelta, L. Riles, C.J. Roberts, P. Ross-MacDonald, B. Scherens, M. Snyder, S. Sookhai-Mahadeo, R.K. Storms, S. Veronneau, M. Voet, G. Volckaert, T.R. Ward, R. Wysocki, G.S. Yen, K. Yu, K. Zimmermann, P. Philippsen, M. Johnston, R.W. Davis, Functional characterization of the *S. cerevisiae* genome by gene deletion and parallel analysis, Science 285 (1999) 901-906.

[19] M. Ikeda, Y. Kanao, M. Yamanaka, H. Sakuraba, Y. Mizutani, Y. Igarashi, A. Kihara, Characterization of four mammalian 3-hydroxyacyl-CoA dehydratases involved in very long-chain fatty acid synthesis, FEBS Lett. 582 (2008) 2435-2440.

[20] A. Kihara, Y. Anada, Y. Igarashi, Mouse sphingosine kinase isoforms SPHK1a and SPHK1b differ in enzymatic traits including stability, localization, modification, and oligomerization, J. Biol. Chem. 281 (2006) 4532-4539.

[21] Y. Kariya, A. Kihara, M. Ikeda, F. Kikuchi, S. Nakamura, S. Hashimoto, C.H. Choi, Y.M. Lee, Y. Igarashi, Products by the sphingosine kinase/sphingosine 1-phosphate (S1P) lyase pathway but not S1P stimulate mitogenesis, Genes Cells 10 (2005) 605-615.

[22] Y. Ohno, A. Ito, R. Ogata, Y. Hiraga, Y. Igarashi, A. Kihara, Palmitoylation of the sphingosine 1-phosphate receptor $S1P_1$ is involved in its signaling functions and internalization, Genes Cells 14 (2009) 911-923.

[23] N. Berndt, S.M. Sebti, Measurement of protein farnesylation and geranylgeranylation *in vitro*, in cultured cells and in biopsies, and the effects of prenyl transferase inhibitors, Nat. Protoc. 6 (2011) 1775-1791.

[24] J. Wan, A.F. Roth, A.O. Bailey, N.G. Davis, Palmitoylated proteins: purification and identification, Nat. Protoc. 2 (2007) 1573-1584.

[25] M. Ikeda, A. Kihara, Y. Igarashi, Sphingosine-1-phosphate lyase SPL is an endoplasmic reticulum-resident, integral membrane protein with the pyridoxal 5'-phosphate binding domain exposed to the cytosol, Biochem. Biophys. Res. Commun. 325 (2004) 338-343.

[26] A. Cátala, Lipid peroxidation of membrane phospholipids generates

hydroxy-alkenals and oxidized phospholipids active in physiological and/or pathological conditions, Chem. Phys. Lipids 157 (2009) 1-11.

[27] S. Wallner, G. Schmitz, Plasmalogens the neglected regulatory and scavenging lipid species, Chem. Phys. Lipids 164 (2011) 573-589.

[28] J.E. Smotrys, M.E. Linder, Palmitoylation of intracellular signaling proteins: regulation and function, Annu. Rev. Biochem. 73 (2004) 559-587.

[29] S. Shahinian, J.R. Silvius, Doubly-lipid-modified protein sequence motifs exhibit long-lived anchorage to lipid bilayer membranes, Biochemistry 34 (1995) 3813-3822.

[30] J.S. Goodwin, K.R. Drake, C. Rogers, L. Wright, J. Lippincott-Schwartz, M.R. Philips, A.K. Kenworthy, Depalmitoylated Ras traffics to and from the Golgi complex via a nonvesicular pathway, J. Cell Biol. 170 (2005) 261-272.

[31] D.A. Mitchell, L. Farh, T.K. Marshall, R.J. Deschenes, A polybasic domain allows nonprenylated Ras proteins to function in *Saccharomyces cerevisiae*, J. Biol. Chem. 269 (1994) 21540-21546.

[32] I. Navarro-Lérida, S. Sánchez-Perales, M. Calvo, C. Rentero, Y. Zheng, C. Enrich, M.A. Del Pozo, A palmitoylation switch mechanism regulates Rac1 function and membrane organization, EMBO J. 31 (2011) 534-551.

[33] Q. Xu, Y.B. Jia, B.Y. Zhang, K. Zou, Y.B. Tao, Y.P. Wang, B.Q. Qiang, G.Y. Wu, Y. Shen, H.K. Ji, Y. Huang, X.Q. Sun, L. Ji, Y.D. Li, Y.B. Yuan, L. Shu, X. Yu, Y.C. Shen, Y.Q. Yu, G.Z. Ju, Association study of an SNP combination pattern in the dopaminergic pathway in paranoid schizophrenia: a novel strategy for complex disorders, Mol. Psychiatry 9 (2004) 510-521.

[34] Y. Wang, Y. Hu, Y. Fang, K. Zhang, H. Yang, J. Ma, Q. Xu, Y. Shen, Evidence of epistasis between the catechol-*O*-methyltransferase and aldehyde dehydrogenase 3B1 genes in paranoid schizophrenia, Biol. Psychiatry 65 (2009) 1048-1054.

[35] A. Yoritaka, N. Hattori, K. Uchida, M. Tanaka, E.R. Stadtman, Y. Mizuno, Immunohistochemical detection of 4-hydroxynonenal protein adducts in Parkinson disease, Proc. Natl. Acad. Sci. USA 93 (1996) 2696-2701.

[36] P.J. Brooks, J.A. Theruvathu, DNA adducts from acetaldehyde: implications for alcohol-related carcinogenesis, Alcohol 35 (2005) 187-193.

[37] K. Shiraishi, K. Naito, Effects of 4-hydroxy-2-nonenal, a marker of oxidative stress, on spermatogenesis and expression of p53 protein in male infertility, J. Urol. 178 (2007) 1012-1017.

[38] P. Fuchs, C. Loeseken, J.K. Schubert, W. Miekisch, Breath gas aldehydes as biomarkers of lung cancer, Int. J. Cancer 126 (2009) 2663-2670.

Figure captions

Fig. 1. Expression of human *ALDH3B1* gene restores the DHS-to-glycerophospholipid metabolism in the Δ*hfd1* yeast mutant. (A) Yeast 6550 (Δ*hfd1*) cells harboring pAKNF316 (vector), pNK10 (*3xFLAG-ALDH3A1*), pNK5 (*3xFLAG-ALDH3A2*), pNK8 (*3xFLAG-ALDH3B1*), or pNK9 (*3xFLAG-ALDH3B2*) were labeled with 0.1 μCi [^{3}H]DHS for 2 h at 30 ˚C. Lipids were extracted, separated by normal-phase TLC with chloroform/methanol/4.2 N ammonia (9:7:2, v/v), and detected by autoradiography. DHS, dihydrosphingosine; DHS1P, dihydrosphingosine 1-phosphate; IPC, inositol phosphorylceramide; MIPC, mannosylinositol phosphorylceramide; M(IP)$_2$C, mannosyldiinositol phosphorylceramide; PC, phosphatidylcholine; PE, phosphatidylethanolamine; PI, phosphatidylinositol; PS, phosphatidylserine. (B) The total lysate was prepared from the cells used in (A) and then subjected to immunoblot analysis with anti-FLAG antibody or, to demonstrate uniform protein loading, with anti-Pgk1 antibody. IB, immunoblotting.

Fig. 2. Overexpression of ALDH3B1 restores the DHS-to-glycerophospholipid metabolism in the *ALDH3A2*-deficient CHO-K1 cells. (A) CHO-K1 cells, FAA-K1A cells, and two FAA-K1A derivatives stably expressing His$_6$-Myc-ALDH3B1 (FAA-ALDH3B1-A and FAA-ALDH3B1-B cells) were labeled with 0.125 μCi [^{3}H]DHS for 4 h at 37 ˚C. Lipids were extracted, treated with nothing or 0.2 M NaOH (followed by neutralization and re-extraction) and separated by normal-phase TLC with 1-butanol/acetic acid/water (3:1:1, v/v). ALDH3B1-A, FAA-ALDH3B1-A; ALDH3B1-B, FAA-ALDH3B1-B; Cer, ceramide; DHS, dihydrosphingosine; GlcCer, glucosylceramide; GPE, glycerophosphoethanolamine;

GPC, glycerophosphocholine; PC, phosphatidylcholine; PE, phosphatidylethanolamine; PI, phosphatidylinositol; PlsC, plasmanylcholine; PlsE, plasmenylethanolamine; PS, phosphatidylserine; SM, sphingomyelin. The asterisk indicates undetermined plasmenylethanolamine degradation products from alkaline treatment. (B) The total lysate (15 μg) prepared from the cells used in (A) was subjected to immunoblot analysis with anti-Myc antibody, or, to demonstrate uniform protein loading, with anti-α-tubulin antibody. IB, immunoblotting.

Fig. 3. ALDH3B1 exhibits activity toward C16 aldehydes. (A) HEK 293T cells were transfected with the pCE-puro 3xFLAG-ALDH3A1, pCE-puro 3xFLAG-ALDH3A2, pCE-puro 3xFLAG-ALDH3B1, or pCE-puro 3xFLAG-ALDH3B2 plasmid. The total lysate prepared from these cells was solubilized with Triton X-100 and subjected to affinity-purification using anti-FLAG M2 beads. The affinity-purified protein (10-20 ng) was incubated with 500 μM NAD^+ and 100 μM hexadecanal for 15 min at 37 ˚C. The fluorescence of the NADH product was measured using monochromator Infinite M200. Values represent the mean ± S.D. from three independent experiments. (B-D) 3xFLAG-ALDH3B1 was affinity purified as in (A), and 3xFLAG-ALDH3B1 (20 ng) was incubated with 500 μM NAD^+ and hexadecanal (10, 33, and 100, and 300 μM) (B), *trans*-2-hexadecenal (3.3, 10, 33, and 100 μM) (C), or octanal (3.3, 10, 33, and 100 μM) (D) for 1.5 min at 37 ˚C. The fluorescence of the NADH product was measured using monochromator Infinite M200. The obtained values were expressed in a Michaelis-Menten plot and a Lineweaver-Burk plot (inset). The units in the inset are μM^{-1} for the x-axis and $pmol^{-1}$ min ng for the y-axis. Values represent the mean ± S.D. from three independent

experiments.

Fig. 4. ALDH3B1 is both prenylated and palmitoylated. (A) HeLa cells were transfected with the pCE-puro 3xFLAG-ALDH3B1 plasmid. Three hours after transfection, cells were incubated with 0, 0.1, 1, and 10 μM geranylgeranyltransferase I inhibitor GGTI-2133 for 48 h at 37 ˚C. The total cell lysate was then prepared by centrifugation at 100,000 x g for 30 min at 4 ˚C. The resulting supernatant (soluble fraction; S) and pellet (membrane fraction; M) were subjected to immunoblotting using anti-FLAG, anti-calnexin (a membrane protein marker), and anti-GAPDH (a soluble protein marker) antibodies. IB, immunoblotting. (B) The C-terminal amino acid sequence (439-468) of human ALDH3B1 is presented. The underlined Cys residues are lipidated. (C) HEK 293T cells were transfected with the pCE-puro 3xFLAG-ALDH3B1, pCE-puro 3xFLAG-ALDH3B1-C463S, pCE-puro 3xFLAG-ALDH3B1-C465S, or pCE-puro 3xFLAG-ALDH3B1-C463/465S plasmid. The total cell lysate was prepared and treated with *N*-ethylmaleimide to block unmodified Cys thiols. The palmitoyl thioester was cleaved with hydroxylamine, and the newly exposed Cys thiol was biotinylated using EZ-Link^{TM} Biotin-HPDP (Thermo Fisher Scientific, Waltham, MA). The biotinylated protein was precipitated with immobilized-avidin beads and detected by immunoblotting with anti-FLAG antibody (upper panel). The ALDH3B1 protein in the total lysate was detected using immunoblotting with anti-FLAG antibody (lower panel). AvP, avidin prercipitation; IB, immunoblotting; WT, wild type.

Fig. 5. Prenylation is required for the plasma membrane localization of ALDH3B1. (A) HeLa cells were transfected with the pEGFP-C1 (vector), pEGFP-ALDH3B1,

pEGFP-ALDH3B1-C463S, pEGFP-ALDH3B1-C465S, or pEGFP-ALDH3B1-C463/465S plasmid. Forty-eight hours after transfection, cells were subjected to microscopic observation under a Leica DM5000B fluorescence microscope (Leica Microsystems, Wetzlar, Germany). Bar, 25 μm. WT, wild type. (B) HeLa cells were transfected with the pCE-puro 3xFLAG-ALDH3B1, pCE-puro 3xFLAG-ALDH3B1-C463S, pCE-puro 3xFLAG-ALDH3B1-C465S, or pCE-puro 3xFLAG-ALDH3B1-C463/465S plasmid. The total cell lysate prepared from these cells was centrifuged at 100,000 x g for 30 min at 4 ˚C. The resulting supernatant (soluble fraction; S) and pellet (membrane fraction; M) were subjected to immunoblotting using anti-FLAG, anti-calnexin (a membrane protein marker), and anti-GAPDH (a soluble protein marker) antibodies. IB, immunoblotting. WT, wild type.

Fig. 6. Prenylation is required for the activity of ALDH3B1 toward hexadecanal. (A) HEK 293T cells were transfected with the pCE-puro 3xFLAG-ALDH3B1, pCE-puro 3xFLAG-ALDH3B1-C463S, pCE-puro 3xFLAG-ALDH3B1-C465S, or pCE-puro 3xFLAG-ALDH3B1-C463/465S plasmid. Each ALDH3B1 protein was affinity-purified from the corresponding TritonX-100-solubilized lysate using anti-FLAG M2 beads, and the purified protein (10-20 ng) was incubated with 500 μM NAD^+ and 100 μM hexadecanal or octanal for 15 min at 37 ˚C. The fluorescence of the NADH product was measured using monochromator Infinite M200. Values represent the mean ± S.D. from three independent experiments. Statistically significant differences are indicated (*$p < 0.05$; t test). (B) Yeast 6550 (Δ*hfd1*) cells harboring pAKNF316 (vector), pNK8 (*3xFLAG-ALDH3B1*), or pTK71 (*3xFLAG-ALDH3B1-C463/465S*) were labeled with 0.1 μCi [^{3}H]DHS for 2 h at 30 ˚C. Lipids were extracted, separated by normal-phase TLC with chloroform/methanol/4.2 N

ammonia (9:7:2, v/v), and detected by autoradiography. Cer, ceramide; DHS, dihydrosphingosine; IPC, inositol phosphorylceramide; MIPC, mannosylinositol phosphorylceramide; $M(IP)_2C$, mannosyldiinositol phosphorylceramide; PC, phosphatidylcholine; PE, phosphatidylethanolamine; PI, phosphatidylinositol; PS, phosphatidylserine; WT, wild type. (C) The total lysate was prepared from the cells used in (B) and subjected to immunoblot analysis with anti-FLAG antibody or, to demonstrate uniform protein loading, with anti-Pgk1 antibody. WT, wild type; IB, immunoblotting.

Supplementary Material and Methods

RNAi and RT-PCR

The pshRNA-Luc and pshRNA-ALDH3B1 plasmids (puromycin marker) encode shRNAs specific for *Luciferase* and *ALDH3B1*, respectively, under the control of *h7SK* promoter. The target sequences for RNAi were 5'-GCGTACGCGGAATACTTCGA-3' (*Luciferase*) and 5'-GAACCCCTGCTATGTGGA-3' (*ALDH3B1*). FAA-K1A cells were transfected either with the pshRNA-Luc or pshRNA-ALDH3B1 plasmids using the Lipofectamine Plus^{TM} Reagent (Invitrogen, Carlsbad, CA). Twenty-four hours after transfection, cells were treated with 10 μg/ml puromycin for 3 h to eliminate untransfected cells. Cells in each dish were then detached by trypsin/EDTA and seeded onto two dishes with medium containing 10 μg/ml puromycin. Two days after the passage (3 days after transfection), the cells in one dish were subjected to [^{3}H]DHS labeling, and those in the other dish were processed to prepare the total RNA using the NucleoSpin RNA II kit (Macherey-Nagel, Düren, Germany) according to the manufacturer's instructions. The *ALDH3B1* and *GAPDH* cDNAs were amplified from the total RNAs using the SuperScript One-Step RT-PCR with Platinum Taq kit (Invitrogen) following the manufacturer's instructions. The nucleotide sequences of primers used were: for *ALDH3B1*, 5'-ATCCGGAAGGAGCCCTTTGGCCTGG-3' and 5'-GTCCAAAGATCTCCTCCTGCATCAC-3', and for *GAPDH*, 5'-CCAAGGTCATCCATGACAACTTTGG-3' and 5'-CCTGCTTCACCACCTTCTTGATGTC-3'.

Supplementary figure caption

Fig. S1. Endogenous ALDH3B1 is not involved in the LCB metabolism in FAA-K1A cells. (A and B) FAA-K1A cells were transfected either with the pshRNA-Luc (control) or pshRNA-ALDH3B1 plasmids, and transfected cells were selected with 10 μg/ml puromycin. (A) Three days after transfection, total RNAs were prepared and subjected to RT-PCR using primers specific for *ALDH3B1* and *GAPDH*. Amplified fragments were separated by agarose gel electrophoresis and stained with ethidium bromide. (B) Three days after transfection, cells were labeled with 0.2 μCi [^{3}H]DHS for 4 h at 37 ˚C. Lipids were extracted and separated by normal-phase TLC with 1-butanol/acetic acid/water (3:1:1, v/v). Cer, ceramide; DHS, dihydrosphingosine; GlcCer, glucosylceramide; PC, phosphatidylcholine; PE, phosphatidylethanolamine; PlsE, plasmenylethanolamine; SM, sphingomyelin.

Figure 1

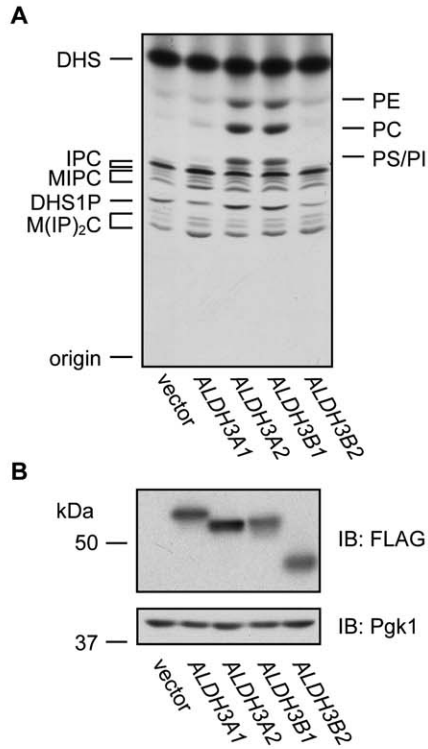
A
DHS
PE
PC
PS/PI
IPC
MIPC
DHS1P
M(IP)2C
origin
vector
ALDH3A1
ALDH3A2
ALDH3B1
ALDH3B2
B
kDa
50
IB: FLAG
37
IB: Pgk1
vector
ALDH3A1
ALDH3A2
ALDH3B1
ALDH3B2

Figure 2

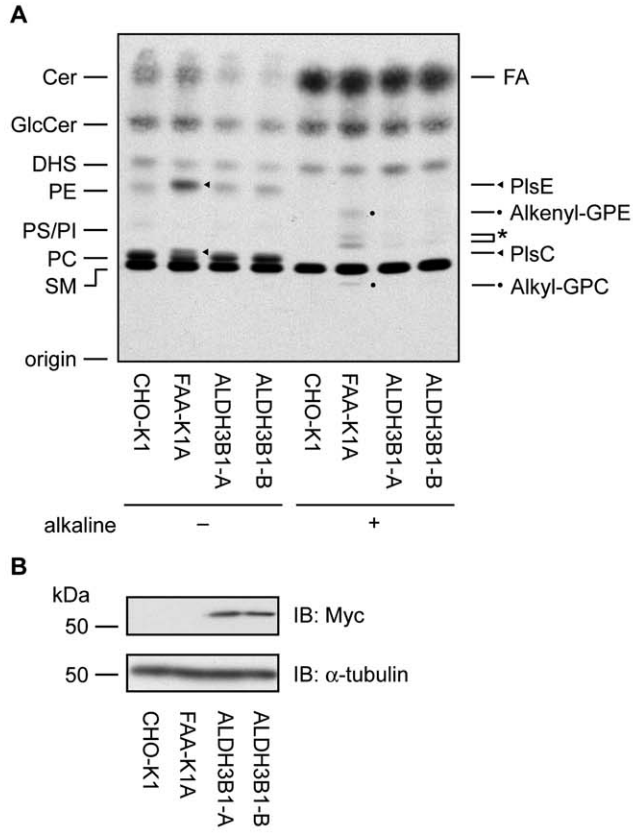
A
Cer
GlcCer
DHS
PE
PS/PI
PC
SM
origin
FA
PlsE
Alkenyl-GPE
PlsC
Alkyl-GPC
CHO-K1
FAA-K1A
ALDH3B1-A
ALDH3B1-B
alkaline
–
+
B
kDa
50
IB: Myc
50
IB: α-tubulin
CHO-K1
FAA-K1A
ALDH3B1-A
ALDH3B1-B

Figure 3

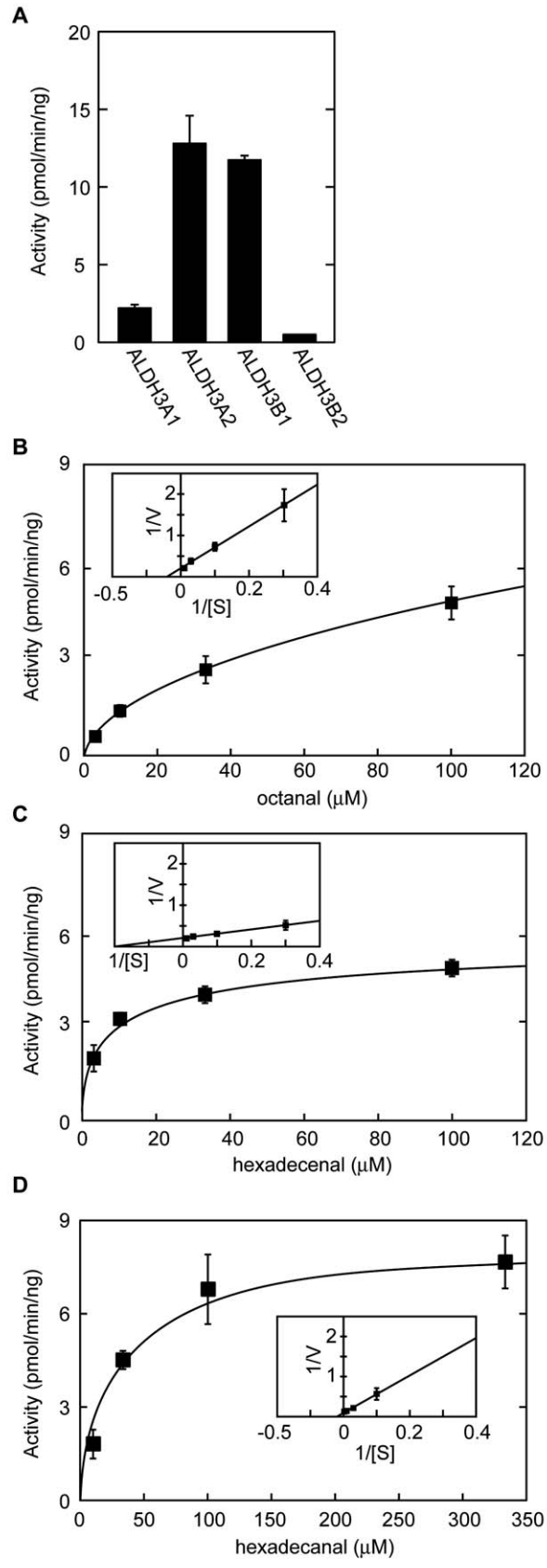
A
Activity (pmol/min/ng)
20
15
10
5
0
ALDH3A1
ALDH3A2
ALDH3B1
ALDH3B2
B
Activity (pmol/min/ng)
octanal (μM)
1/V
1/[S]
C
Activity (pmol/min/ng)
hexadecenal (μM)
1/V
1/[S]
D
Activity (pmol/min/ng)
hexadecanal (μM)
1/V
1/[S]

Figure 4

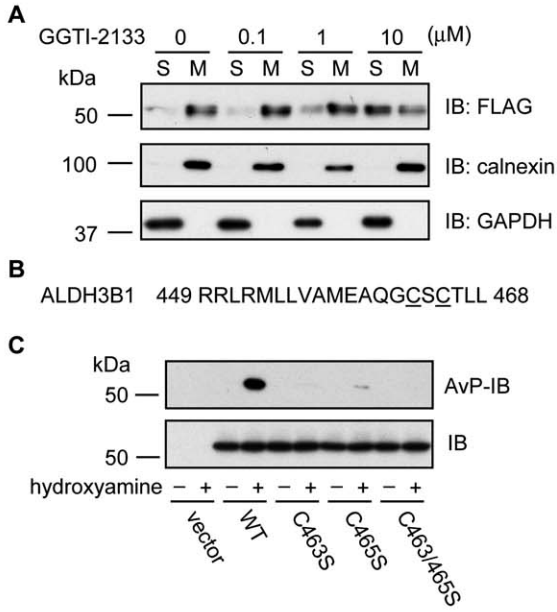
A
GGTI-2133 0 0.1 1 10 (μM)
S M S M S M S M
kDa
50
IB: FLAG
100
IB: calnexin
37
IB: GAPDH
B
ALDH3B1 449 RRLRMLLVAMEAQGCSCTLL 468
C
kDa
50
AvP-IB
50
IB
hydroxyamine − + − + − + − + − +
vector
WT
C463S
C465S
C463/465S

Figure 5

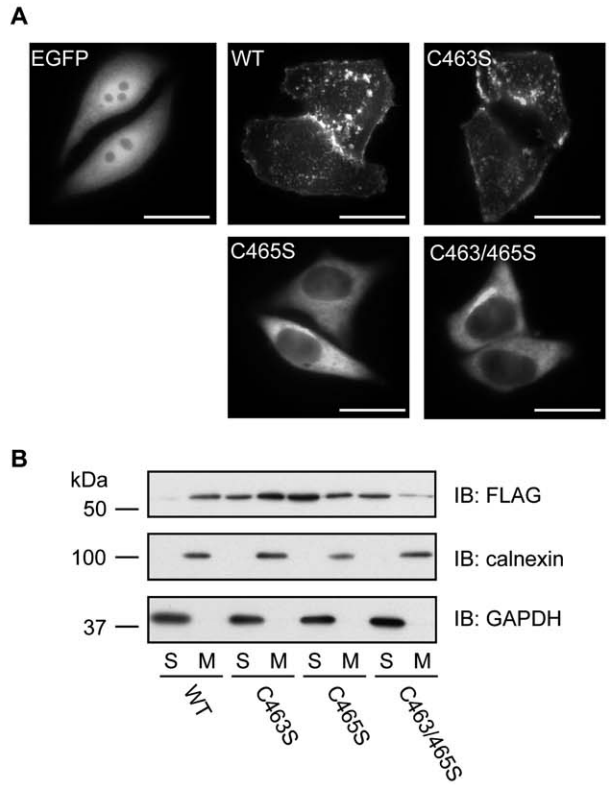
A
EGFP
WT
C463S
C465S
C463/465S
B
kDa
50
100
37
IB: FLAG
IB: calnexin
IB: GAPDH
S M S M S M S M
WT
C463S
C465S
C463/465S

Figure 6

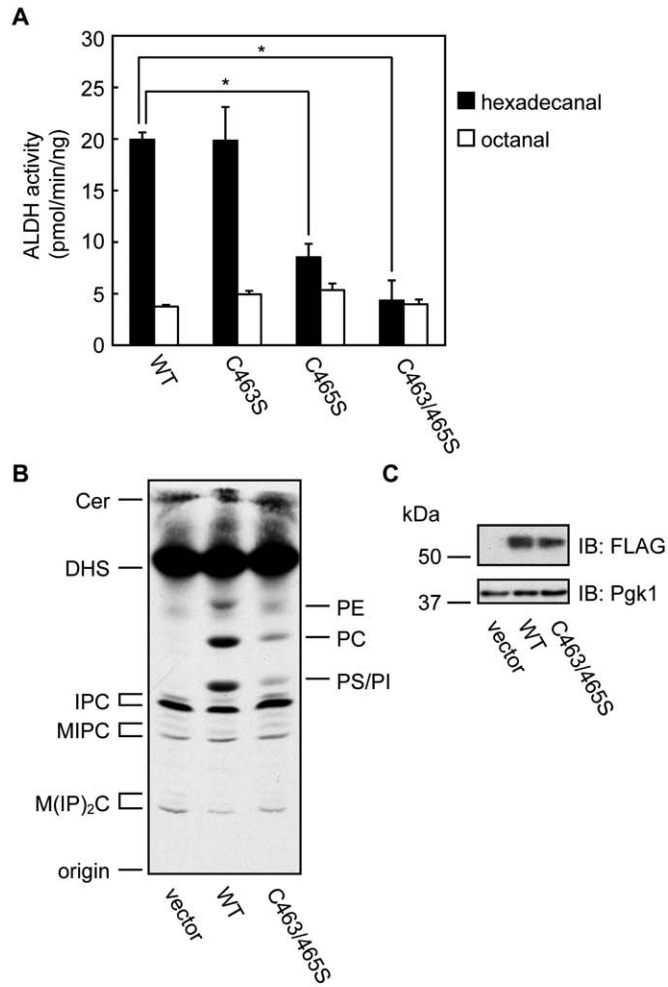
A
ALDH activity (pmol/min/ng)
30
25
20
15
10
5
0
*
*
hexadecanal
octanal
WT
C463S
C465S
C463/465S
B
Cer
DHS
IPC
MIPC
M(IP)2C
origin
PE
PC
PS/PI
vector
WT
C463/465S
C
kDa
50
37
IB: FLAG
IB: Pgk1
vector
WT
C463/465S

Figure S1

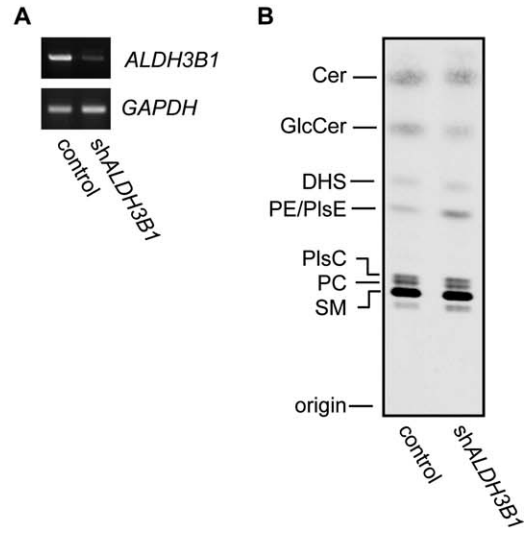
A
ALDH3B1
GAPDH
control
shALDH3B1
B
Cer
GlcCer
DHS
PE/PlsE
PlsC
PC
SM
origin
control
shALDH3B1